Chinese Chemical Letters 33 (2022) 3484–3487

Contents lists available at ScienceDirect

Chinese Chemical Letters

journal homepage: www.elsevier.com/locate/cclet

Laser ablation-single particle-inductively coupled plasma mass spectrometry as a sensitive tool for bioimaging of silver nanoparticles *in vivo* degradation

Meng Wang[a], Lingna Zheng[a], Bing Wang[a], Pu Yang[a,b], Hao Fang[a,b], Shanshan Liang[a,b], Wei Chen[a,b], Weiyue Feng[a,*]

[a] *CAS Key Laboratory for Biomedical Effects of Nanomaterials and Nanosafety, Institute of High Energy Physics, Chinese Academy of Sciences, Beijing 100049, China*

[b] *University of Chinese Academy of Sciences, Beijing 100049, China*

ARTICLE INFO

Article history:
Received 17 January 2022
Revised 22 March 2022
Accepted 23 March 2022
Available online 26 March 2022

Keywords:
LA-sp-ICP-MS
Silver nanoparticle
Bioimaging
Degradation

ABSTRACT

The *in vivo* degradation behavior of metallic nanoparticles (NPs) is very important for their biomedical applications and safety evaluation. Here, a method of laser ablation-single particle inductively coupled plasma mass spectrometry (LA-sp-ICP-MS) is shown to have high spatial resolution, sensitivity and accuracy for simultaneous imaging the *in situ* distribution of particulate Ag (P-Ag) and released ionic Ag (Ion-Ag) in the sub-organs of spleen, liver and kidney after intravenous injection of Ag nanoparticles (50 nm, AgNPs) to mice. Under the optimized parameters of 0.4 J/cm^2 laser fluence on a 30 μm spot with dwell time at 100 μs, the signals of P-Ag and Ion-Ag in the organic tissues can be easily distinguished from the mass spectra. The method of iterative threshold algorithm has been used to distract the signals of P-Ag and Ion-Ag and separate each other. The resulting images for the first time provide visualized evidence that a considerable amount of P-Ag accumulated in the splenic marginal zone, but widely distributed in the liver parenchyma at 24 h after injection of AgNPs, and in the meantime, obvious amounts of ionic Ag released and distributed in the organs. In addition, the imaging results indicate that the AgNP excretion in the kidney is mainly in ionic forms. The investigation here demonstrates that the developed LA-sp-ICP-MS method with high spatial resolution, sensitivity and visualization capability can become a powerful tool in the clinical context of metallic NPs.

Metal-based nanoparticles (NPs), such as silver NPs, gold NPs and metallic oxide (zinc oxide, copper oxide, iron oxide, *etc.*) NPs due to their unique physiochemical properties of strong antibacterial activity, optical polarizability, electrical conductivity, biocompatibility, are promising applied in agri-food industry, environmental remediation and a set of biomedical applications, *etc.* [1–3]. However, in the meanwhile, metallic NPs raise great concerns about their ecological exposure and the potentially adverse effects on human health. The toxicity mechanisms of metallic NPs are not yet fully understood. It is now widely recognized that the conformational changes by aggregation, dissolution and chemical transformation of NPs have high association with their toxicity, among those, dissolution was found to play an important role, but to what extent affecting their toxicity remains unclear. One of the reasons is that characterization the particulate and ionic statues of metallic NPs in biological system is a prime challenge.

To explore the effects of ion release and the toxicity mechanism of NPs on living systems, the method that could simultaneously identify and determine ionic and particulate forms of metals in biological tissues, further, imaging their distributions to *in situ* assess those changes, is urgently required. Though many kinds of analytical techniques such as X-ray absorption spectroscopy (XAS), X-ray photoelectron spectroscopy (XPS), Fourier transform infrared (FTIR) spectroscopy, can be used to identify valent, surface ligand or the coordination sphere changes of central metals in a sample, but none of them could offer sensitive *in vivo* imaging of both ionic and particulate forms of NPs. Currently, an analytical technique based on a combination of laser ablation sampling technique with single particle inductively coupled plasma mass spectrometry (LA-sp-ICP-MS) has been used to simultaneously imaging the size and position of NPs in plants [4–6]. Metarapi *et al.* [5] originally imaged gold NPs in root cross sections of sunflower plants

* Corresponding author.
E-mail address: fengwy@ihep.ac.cn (W. Feng).

https://doi.org/10.1016/j.cclet.2022.03.098
1001-8417/

using LA-sp-ICP-MS (an Analyte G2, 193 nm ArF coupled with Agilent 7900 ICP-MS, Agilent Technologies, Santa Clara, CA) and offered a proof-of-concept that the method could distinguish NPs in a size-mixed mixture. Further, using LA-sp-ICP-MS, they obtained multiplexed images of Ag^+ and AgNPs with the tissue-level resolution and demonstrated that the uptake of Ag^+ had transformed to AgNPs in the root cross-sectional regions of sunflower [5]. Yamashita *et al.* [4] simultaneously determined the size and position of Ag and Au NPs in onion cells by the method of LA-sp-ICP-MS, which was performed with 193 nm excimer-based laser ablation system (Analyte Excite, Teledyne Cetac, Omaha, USA) coupled with a magnetic sector ICP-MS (AttoM, Nu Instruments, Wrexham, UK). However, no such detections have been yet performed in mammalian tissues that may reflect the endogenous biotransformation of nanoparticles.

In the study, a high-performance Nd:YAG deep UV (213 nm) laser ablation system coupled to sp-ICP-MS has been shown as a powerful imaging tool to visualize the *in situ* distribution features of particulate Ag (P-Ag) and the released ionic Ag (Ion-Ag) in the target organs. Over the years, with the increasing use of AgNPs in numerous healthcare, biomedical and consumer products, serious concerns have been raised about their adverse effects [7–9]. It has been widely accepted that the release of silver ion (Ag^+) from AgNPs is one of the crucial factors contributing to AgNP cytotoxic activity. Many researches have shown that the Ag^+ release is dependent on several factors including the nanoparticle size, shape, concentration, chemical surface, *etc.*, and its present environment where contains chlorine, thiols, sulfur, oxygen, *etc.* [7,10,11]. However, so far, the behaviors of Ag^+ release from AgNPs are predominately obtained from the *in vitro* analysis. The *in vivo* release that would be highly affected by the biological microenvironment has not been known yet. Herein, by using the performed LA-sp-ICP-MS, we show that a considerable amount of both P-Ag and Ion-Ag accumulated within the target organs of spleen, liver and kidney after the mice receiving a single intravenous (iv) injection of AgNP suspension, suggesting both the two forms of silver might contribute to the biological/toxic effects. We demonstrate the promising that the LA-sp-ICP-MS with high spatial resolution, sensitivity and visualization can expand to provide key information of the uptake, translocation and degradation features of the metallic NPs in the living system.

In the work, the single particle ICP-MS (sp-ICP-MS) measurements were performed using a quadrupole ICP-MS (NexION 300D, PerkinElmer, Inc., USA) equipped with a high-efficiency sample introduction system which was constructed in our laboratory with favorable efficiency for single particle or single cell measurement [12–15]. The sample introduction system includes a HEN microconcentric nebulizer (Meinhard, USA), a low-volume, single pass spray chamber (Viktor Beijing Technology Co., Ltd. China), and a SP120PZ syringe pump (World Precision Instruments, UK). The transport efficiency of single particles can be reached to more than 12%. The typical instrumental parameters for sp-ICP-MS are shown in Table 1.

The LA-sp-ICP-MS imaging analysis was carried out using an NWR213 laser ablation system (ESI, Fremont, CA U.S.) coupled to the sp-ICP-MS. The laser ablation system equipped with a high-performance Nd:YAG deep UV (213 nm) laser and a two-volume ablation cell that ensures fast wash-in and wash-out of the aerosol in the cell, as well as excellent signal stability. The LA-sp-ICP-MS system was optimized using NIST 612 standard glass, achieving high sensitivity for $^{115}In^+$ and low percentages of oxides and double charged ions before use. The standards of AgNPs with size of 50, 60 and 80 nm were used in the study. The preparation of gelatin calibration standards of P-Ag and Ion-Ag are described in the supporting information. The parameters of dwell time for sp-ICP-MS accurate analysis of particulates and the laser fluence for complete ablation of tissue slice were optimized (Supporting information). The operation parameters for LA-sp-ICP-MS imaging analysis of P-Ag and Ion-Ag are shown in Table 1. The images were produced using the Igor Pro 6.10 software.

Table 1
Typical operation parameters for AgNPs analysis by sp-ICP-MS.

Laser ablation (LA) system: Nd:YAG laser (λ = 213 nm)	
He gas flow (L/min)	0.7
Laser fluence (J/cm^2)	0.4–3.5
Spot size (μm)	30
Scan speed (μm/s)	30
Repetition frequency (Hz)	20
Ablation mode	line
Distance between lines (μm)	50
sp-ICP-MS	
Carrier gas	Ar
Nebulizer gas flow (L/min)	1.0
Auxiliary gas flow (L/min)	1.2
Plasma gas flow (L/min)	18.0
RF Power (W)	1600
Dwell time (ms)	0.05∼5
Data acquisition (s)	60
Isotope determined	^{107}Ag

The sp-ICP-MS in a time-resolved manner is a rapid and continuous measurement with microsecond data acquisition rate, so the LA-sp-ICP-MS for ^{107}Ag imaging of tissues will produce a large volume of data. In the study, the scan area is generally 2×1 mm^2. The raw data (total-Ag) are the mixture with the signals from both P-Ag and Ion-Ag. To identify each of the signal and separate the P-Ag signals from Ion-Ag ones, a pre-process to define the threshold of Ion-Ag signal should be done first.

Under the sp-ICP-MS measurement, the mass spectrum of P-Ag presents discrete pulses of ^{107}Ag signals, while the Ion-Ag shows a steady-state signal. For the short integration time of 100 μs, the background noise is very low and follows the Poisson statistics [16–18]. The following threshold was used:

$$\text{Threshold} = \text{mean} + 3.29\sigma_{\text{blank}}(\text{counts}) + 2.71 \quad (1)$$

The accuracy and detection limits of LA-sp-ICP-MS for P-Ag and Ion-Ag detection were obtained from the gelatin film standards of P-Ag, Ion-Ag and the mixed-species measurements (Figs. S4 and S5 in Supporting information). After the P-Ag and Ion-Ag signals had been identified and separated from the total $^{107}Ag^+$ signal, the data points of each other were integrated and subjected to the Igor pro 6.10 software to draw P-Ag and Ion-Ag images separately.

For sp-ICP-MS analysis, theoretically, when a dilute particle suspension is introduced at a low flow rate into the plasma, each discrete particle will be vaporized, atomized and a burst of ions will be generated. Using ICP-MS in time resolved mode, the resulting signal is related to the size of the particle and the number of pulses is related to the particle concentration [17,18]. Under the sp-ICP-MS operating model, the mass spectrum of ions in solution is present as a steady-state signals, whereas, the particles in suspension solution shows discrete pulse signals (as shown in Fig. 1).

LA-sp-ICP-MS further allows detection of particles for the *in situ* size calibrations and particle counting in the sample [6]. When the sample is mixed with particles and dissolved elements, the sp-ICP-MS may perform as a multimodal detection technique for simultaneous measurement of particles and ions with location information. Fig. 1 shows the mass spectra of the gelatin standard slices containing mixed 50 nm-AgNPs (8.37×10^8/mL) and ionic Ag^+ (0, 0.5, 1, 2, 5 mg/L) by LA-sp-ICP-MS scan detection. It can be observed that the baseline obviously elevated with the increase of Ag^+ in the gelatin, however, the intensity of AgNPs is much higher than that of ionic Ag^+, from several fold to several dozen fold high, indicating the signals of ionic Ag^+ and AgNPs can be separately

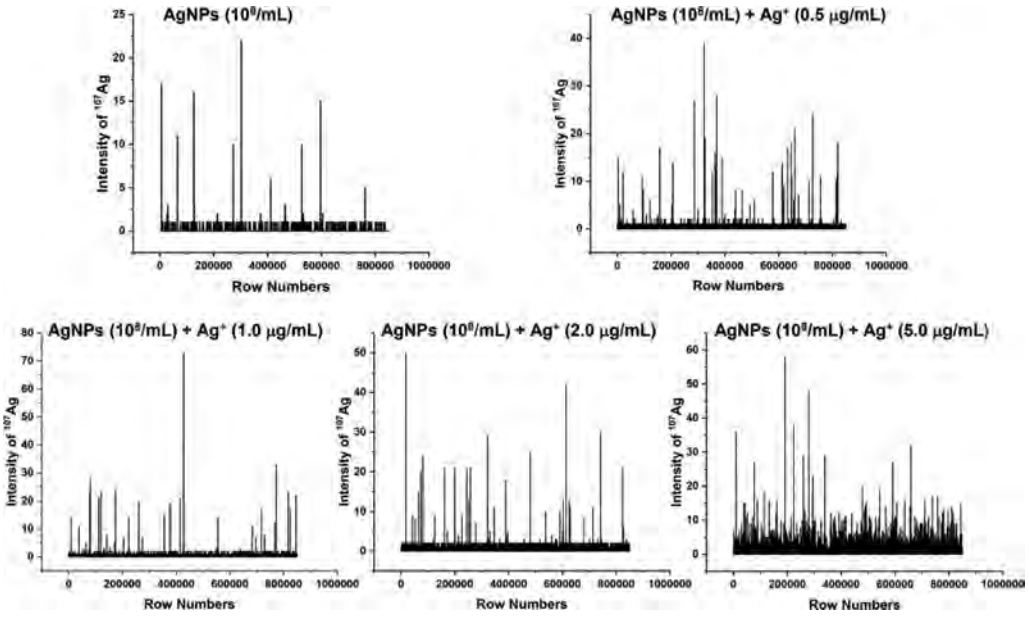

Fig. 1. The mass spectra of gelatin standards containing 50 nm AgNPs (8.37×10^8/mL) and Ag^+ (0, 0.5, 1, 2, 5 mg/L) obtained by LA-sp-ICP-MS line-scan detection.

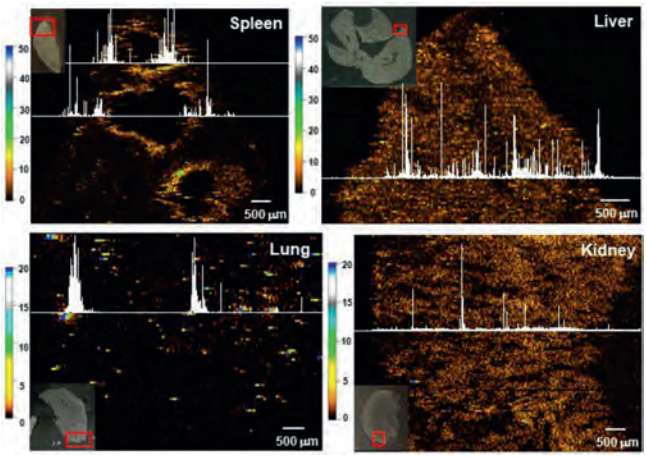

Fig. 2. Using LA-sp-ICP-MS to imaging total-Ag in the spleen, liver, kidney and lung at 24 h after mice iv injection of AgNPs at a dose of 3 mg/kg bw.

identified. In the work, the iterative algorithm is performed on the baseline recognized previously [17,19]. In short, firstly, three times the standard deviation (3σ) of all the points of blank or the pure ionic Ag^+ was initialized, and then the data points of ^{107}Ag exceeding the mean intensity plus 3σ of blank was used to filter Ion-Ag and P-Ag signals, further, the threshold according to Eq. 1 was used to distinguish the P-Ag signals from the Ion-Ag ones.

Finally, the simultaneous imaging of P-Ag and Ion-Ag distribution in mouse organs by LA-sp-ICP-MS has been performed. The details of animal experiments are described in Supporting information. The mice ($n = 6$) were intravenously injected 200 μL AgNP suspension solution at dose of 0.03 μg/g bw. At 24 h post-injection, the organ samples of liver, lung, spleen and kidney were harvested. All animal experiments were reviewed and approved by the Institutional Animal Ethics Committee.

By using LA-sp-ICP-MS, the AgNP interception in the reticuloendothelial system (RES) of spleen, liver, lung and excretion in the kidney were visually analyzed (Fig. 2). The imaging method was optimized with the conditions described above. The images of total-Ag are sensitive enough and have high spatial resolution that an image has a pixel size of 2×1 mm^2 by the parallel adjoining line-scans contains more than 7.2×10^7 data points, thus Ag distributions in the sub-organs can be visualized. Especially, the image of the spleen shows that total-Ag was specifically accumulated at the border between splenic red and white pulp, *i.e.*, the marginal zone (MZ) region, which is consistent with the findings of nanoparticle *in vivo* distributions in the previous works [20,21]. Whereas, the total-Ag shows broader distributions in the liver and kidney, though the high-resolution images show that in the blood vessel regions or the interstitial space, the intensities of Ag signals are low. Very little amount of Ag accumulation is observed in the lung at 24 h after a single iv injection of the AgNPs.

According to the established threshold by Eq. 1 for identification of P-Ag and Ion-Ag, the data points of P-Ag and Ion-Ag were distracted and integrated, then the separate P-Ag and Ion-Ag images of the spleen, liver and kidney were drawn (Fig. 3). The images show interesting evidence that the P-Ag and Ion-Ag presented markedly different distribution features in the organic tissues. In the spleen, P-Ag obviously accumulated around MZ, while the released ionic Ag, *i.e.*, Ion-Ag, homogenously distributed in the red pulp, moreover, both P-Ag and Ion-Ag rarely accumulated in the white pulp. However, differently from in the spleen, both P-Ag and Ion-Ag show homogenous distribution in the liver, while P-Ag image show obvious low intensity of ^{107}Ag signal in the central vein or liver sinusoid. In contrast, in the kidney, very low content of P-Ag was visualized, meanwhile, most of the Ag was present as Ion-Ag in the renal cortex at 24 h after injection of AgNPs.

Though many researches have demonstrated that AgNP cellular internalization and release of Ag^+ is the major cause of AgNP-induced toxicity in the living system [22–24], it is not yet clear whether the *in vivo* distribution and toxic impact were due to its particulate forms, ionic species, or the combination of the two [25,26]. In the study, the P-Ag and Ion-Ag distribution images clearly show that even at 24 h after AgNP injection, though the obvious amounts of ionic Ag predictably released and stored in the organs, a considerable content of particulate forms present in the spleen and liver, inferring the P-Ag contribution to the effects. Sufficient evidence shows that AgNP interactions with biological media and biomolecules lead to particle agglomeration or aggregation when AgNPs enter living system [22,27,28], therefore, cellular uptake and biological transformation are defined by the agglomera-

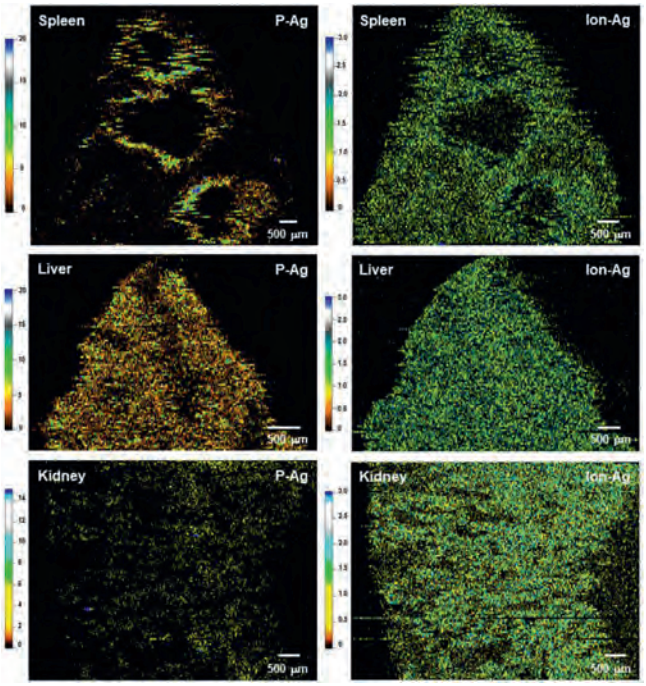

Fig. 3. Using LA-sp-ICP-MS to simultaneously imaging particulate Ag (P-Ag) and ionic Ag (Ion-Ag) distribution in the spleen, liver and kidney at 24 h after mice iv injection of AgNPs at a dose of 3 mg/kg bw.

tion state of AgNPs. So far, less is known about AgNP chemical transformations in the body. Liu *et al.* [23] based on the *in vitro* AgNP transformation study in biological media, proposed that *in vivo* AgNPs would under complex change processes including partially dissolution, systemic circulation as organo-Ag complexes *via* thiol binding, forming secondary particles by photoreduction, or forming Ag_2S solid phases *via* selenide exchange. Loeschner *et al.* [28] reported the deposition of selenium- and sulfur-contained silver granules in the small intestine, liver, and kidney tissues after rat oral exposure of AgNPs (~14 nm). Malysheva *et al.* [7] with sp-ICP-MS measurement demonstrated that intracellular Ag present in nanoparticulate form in the 24 h AgNP-exposed human lymphocytes. Based on the imaging results and the previous researches [24–26], we proposed that the P-Ag observed in the organs might contain the original AgNPs, the aggregated AgNPs and the secondary Ag particulates such as Ag_2S or other large ligand coated P-Ag complexes. The component of Ion-Ag in the organs probably includes various small Ag-containing molecules and very small nano-sized Ag colloids, of which the size is below the detection limit of LA-sp-ICP-MS.

The significant finding in the image results is that a great amount and high release rate of ionic Ag broadly infiltrate in the organic tissues, inferring the Ag^+ rapidly and actively interacting with biological molecules that induces toxicity. Notably, the homogenous distribution of Ion-Ag in the kidney indicates the fast excretion rate of released Ag from AgNPs, thus the potential risk of Ion-Ag induced renal toxicity should be noticed.

In summary, we have shown that the LA-sp-ICP-MS method with high spatial resolution can be used as an powerful tool for simultaneously and accurately imaging the *in situ* distribution of particulate form of Ag (P-Ag) and ionic form of Ag (Ion-Ag) in the animal sub-organs. The *in situ* images for the first time show us specific features of P-Ag and Ion-Ag distributions in the sub-organs of the spleen, liver and kidney after single iv injection of 50 nm AgNPs to mice. Finally, the imaging results provide visualized evidence that both the P-Ag and Ion-Ag may all contribute to the biological/toxic effects in the organs such as the spleen and liver. The kidney images demonstrate that the Ion-Ag is more moveable than P-Ag that most amount of Ag in the kidney are ionic forms.

Collectively, the developed LA-sp-ICP-MS method with high sensitivity, high spatial resolution and visualization capability can provide key information about the uptake, translocation and degradation features of the metallic NPs in the body, which are very important for the development of safety and efficacy nanomedicine.

Declaration of competing interest

All authors of the manuscript titled "Laser ablation-single particle-inductively coupled plasma mass spectrometry as a sensitive tool for bioimaging of silver nanoparticles *in vivo* degradation" declare that they have no conflict of interest.

Acknowledgment

This work was supported by the National Natural Science Foundation of China (Nos. 11975251, 11875268).

Supplementary materials

Supplementary material associated with this article can be found, in the online version, at doi:10.1016/j.cclet.2022.03.098.

References

[1] M. Kah, R.S. Kookana, A. Gogos, T.D. Bucheli, Nat. Nanotechnol. 13 (2018) 677–684.
[2] L.M. Stabryla, K.A. Johnston, N.A. Diemler, et al., Nat. Nanotechnol. 16 (2021) 996–1003.
[3] N.K. Younis, J.A. Ghoubaira, E.P. Bassil, et al., Nanomedicine 36 (2021) 102433.
[4] S. Yamashita, Y. Yoshikuni, H. Obayashi, et al., Anal. Chem. 91 (2019) 4544–4551.
[5] D. Metarapi, J.T. van Elteren, M. Šala, et al., Environ. Sci. Nano 8 (2021) 647–656.
[6] D. Metarapi, M. Šala, K. Vogel-Mikuš, et al., Anal. Chem. 91 (2019) 6200–6205.
[7] A. Malysheva, A. Ivask, C.L. Doolette, et al., Nat. Nanotechnol. 16 (2021) 926–932.
[8] C. Recordati, M. De Maglie, S. Bianchessi, et al., Part. Fibre Toxicol. 13 (2016) 12.
[9] N. Feliu, D. Docter, M. Heine, et al., Chem. Soc. Rev. 45 (2016) 2440–2457.
[10] C. Liu, W. Leng, P.J. Vikesland, Environ. Sci. Technol. 52 (2018) 2726–2734.
[11] L. Wang, T. Zhang, P. Li, et al., ACS Nano 9 (2015) 6532–6547.
[12] J. Liu, L. Zheng, J. Shi, et al., At. Spectrosc. 42 (2021) 114–119.
[13] L.N. Zheng, M. Wang, B. Wang, et al., Talanta 116 (2013) 782–787.
[14] M. Wang, L.N. Zheng, B. Wang, et al., Anal. Chem. 86 (2014) 10252–10256.
[15] L.N. Zheng, L.X. Feng, J.W. Shi, et al., Anal. Chem. 92 (2020) 14339–14345.
[16] O. Borovinskaya, S. Gschwind, B. Hattendorf, et al., Anal. Chem. 86 (2014) 8142–8148.
[17] H. Wang, B. Wang, M. Wang, et al., Analyst 140 (2015) 523–531.
[18] H. Wang, M. Wang, B. Wang, et al., Anal. Bioanal. Chem. 409 (2017) 1415–1423.
[19] J. Tuoriniemi, G. Cornelis, M. Hassellöv, Anal. Chem. 84 (2012) 3965–3972.
[20] L. Newman, D.A. Jasim, E. Prestat, et al., ACS Nano 14 (2020) 10168–10186.
[21] X. Li, H. Yu, B. Wang, et al., ACS Biomater. Sci. Eng. 7 (2021) 1462–1474.
[22] V. De Matteis, M.A. Malvindi, A. Galeone, et al., Nanomedicine 11 (2015) 731–739.
[23] J. Liu, Z. Wang, F.D. Liu, et al., ACS Nano 6 (2012) 9887–9899.
[24] A. Malysheva, A. Ivask, C.L. Doolette, et al., Nat. Nanotechnol. 16 (2021) 926–932.
[25] Z. Ferdous, A. Nemmar, Int. J. Mol. Sci. 21 (2020) 2375.
[26] E.O. Mikhailova, J. Funct. Biomater. 11 (2020) 84.
[27] A. Lankoff, W.J. Sandberg, A. Wegierek-Ciuk, et al., Toxicol. Lett. 208 (2012) 197–213.
[28] K. Loeschner, N. Hadrup, K. Qvortrup, et al., Part. Fibre Toxicol. 8 (2011) 18.